Preprints.org

Article

Not peer-reviewed version

Performance of An Energy Production System Consisting of Solar Collector, Biogas Dry Reforming Reactor and Solid Oxide Fuel Cell

Akira Nishimura * , Ryotaro Sato , Eric Hu

Posted Date: 29 January 2024

doi: 10.20944/preprints202401.1909.v1

Keywords: Solar Collector; Weather Data; Japanese Cities; Biogas Dry Reforming; H2 Production; SOFC

Preprints.org is a free multidiscipline platform providing preprint service that is dedicated to making early versions of research outputs permanently available and citable. Preprints posted at Preprints.org appear in Web of Science, Crossref, Google Scholar, Scilit, Europe PMC.

Copyright: This is an open access article distributed under the Creative Commons Attribution License which permits unrestricted use, distribution, and reproduction in any medium, provided the original work is properly cited.

Preprints.org (www.preprints.org) | NOT PEER-REVIEWED | Posted: 29 January 2024 doi:10.20944/preprints202401.1909.v1

Disclaimer/Publisher's Note: The statements, opinions, and data contained in all publications are solely those of the individual author(s) and contributor(s) and not of MDPI and/or the editor(s). MDPI and/or the editor(s) disclaim responsibility for any injury to people or property resulting from any ideas, methods, instructions, or products referred to in the content.

Article

Performance of An Energy Production System Consisting of Solar Collector, Biogas Dry Reforming Reactor and Solid Oxide Fuel Cell

Akira Nishimura [1,*], Ryotaro Sato [1] and Eric Hu [2]

[1] Mie University; nisimura@mach.mie-u.ac.jp
[2] the University of Adelaide; eric.hu@adelaide.edu.au
* Correspondence: nisimura@mach.mie-u.ac.jp; Tel.: +81-59-231-9747

Abstract: This paper aims to study the performance of solar collectors with various sizes under different weather conditions of different Japanese cities, i.e. Kofu city, Nagoya city and Yamagata city. The heat generated from the solar collector was used to conduct a biogas dry reforming reactor in order to produce H_2 to feed a solid oxide fuel cell (SOFC). This study has revealed that the output temperature of solar collector, T_{fb} in April and July was higher than that in January and October irrespective of city. The optimum length of absorber (dx) of the collector was 4 m irrespective of city. It was clarified that T_{fb} in Yamagata city in January and October, i.e. winter and autumn is lower than that in Kofu city and Nagoya city especially, which is influenced by the tendency of a solar intensity (I) strongly, not velocity of surrounding air (u_a). On the other hand, T_{fb} is almost the same in April and July, i.e. spring and summer, irrespective of city. The amount of produced H_2 from the biogas dry reforming reactor and the power generated by SOFC using H_2 in spring and summer were higher compared to the other seasons irrespective of city. This study has revealed that the highest available households number per month was 4.7 according to the investigation in this study.

Keywords: solar collector; weather data; Japanese cities; biogas dry reforming; H_2 production; SOFC

1. Introduction

Global warming is an important issue for the world. One of promising approaches is a renewable energy. According to Energy White Paper [1], the ratio of installment capacity of renewable energy excluding hydropower generation to the whole energy is 20.7 % in the world in 2020. In addition, the ratio of power energy of renewable energy excluding hydropower generation to the whole energy is 12.2 % in the world in 2022. World Energy Outlook 2022 forecasts that the ratio of power energy of renewable energy to the whole energy will increase up to 49 % in 2030 [2]. Therefore, it is necessary to promote the renewable energy utilization more.

To reduce CO_2 which is a main chemical to cause the global warming, H_2 is paid attention in the world. This study focuses on the H_2 production from biogas dry reforming reaction process. Biogas consisting of CH_4 (55 - 75 vol%) and CO_2 (25 – 45 vol%) [3] is produced from fermentation by the action of anaerobic micro-organisms on raw materials such as garbage, livestock and sewage sludge. According to the International Energy Agency (IEA) [4], 1.46 EJ equivalent biogas has been produced in 2020. The amount of energy of produced biogas in 2020 is approximately five times as large as that in 2000. It can be expected that the produced biogas will increase more. Therefore, the biogas is a promising energy source. Though the biogas is used as a fuel for gas engine or micro gas turbine generally [5], the efficiency of power generation decreases compared to using a natural gas. Since a biogas contains CO_2 of approximately 40 vol%, the heating value of biogas is smaller compared to that of natural gas. In this study, biogas is proposed to be used as feedstock to produce H_2 through thermally powered biogas dry reforming process. The H_2 can be used as a fuel for solid oxide fuel cell (SOFC) [6]. SOFC can also use CO which is a by-product from biogas dry reforming as a fuel, resulting that the effective energy production system can be realized.

© 2024 by the author(s). Distributed under a Creative Commons CC BY license.

Preprints.org (www.preprints.org) | NOT PEER-REVIEWED | Posted: 29 January 2024 doi:10.20944/preprints202401.1909.v1

This study proposes the system combining the above mentioned energy production system with a solar collector to supply the heat required since the biogas dry reforming is an endothermic reaction. Some studies previously reported the combined system to produce H_2 using the solar collector in order to provide the heat for the chemical reaction. The parabolic trough solar collector (PTC) has been investigated for this purpose for CH_3OH steam reforming [7-11]. Numerical analysis using the commercial software COMSOL and Fluent has been conducted to evaluate the H_2 production performance, the temperature distribution and the thermal efficiency of the combination system [7, 8, 10, 11]. The other numerical thermodynamic analysis has been investigated on the solar CH_4 steam reforming with H_2 permeation membrane reactors [12]. In this study [12], the PTC was adopted to provide the heat for CH_4 steam reforming. The distribution of partial pressure of each gas, conversion rate of CH_4 and H_2O and thermodynamic efficiency were calculated changing the reaction temperature from 573 K to 873 K, resulting that the amount of produced H_2 and the thermodynamic efficiency are the largest at 873 K. The thermodynamic efficiency up to 70 % could be obtained. Regarding the combination system to produce H_2 using the solar collector in order to provide the heat for CH_4 dry reforming including biogas dry reforming, several studies have been reported [13-15]. Zhao *et al*. [13] has reported the analysis results of the thermodynamic performance, indicating that the conversion rate of CH_4 as well as the CO_2 emission reduction increase with the reaction temperature. According to the combination of thermodynamic analysis and regression analysis for steam and dry CH_4 reforming [14], the CH_4 conversion increased with the reaction temperature exponentially from 470 K to 870 K. On the other hand, according to the experimental study on the combination system to produce H_2 using the solar collector in order to provide the heat for CH_4 dry reforming including biogas dry reforming, the volume percentage of produced H_2 increased with the reaction temperature from 623 K to 1273 K. The volume percentage of H_2 attained 45 % at 1273 K. It was reported that the lower heating value of produced syngas could exceed that of input biogas over 673 K.

However, there is no study to investigate the impact of size of solar collector on the temperature of biogas which flows through the solar collector and the performance to produce H_2 from biogas dry reforming reactor and the power generated by SOFC excluding the authors' previous study [6]. In addition, the feasibility study using the weather data to investigate the performance of solar collector as well as producing H_2 from biogas dry reforming reactor and the power generated by SOFC was not reported excluding the authors' previous study [6]. However, the authors' previous study has not investigated the impact of weather data for the different cities in Japan on the performance of solar collector as well as producing H_2 from biogas dry reforming reactor and the power generated by SOFC. Since the feasibility study to install the combination system consisting of solar collector, biogas dry reforming reactor and SOFC for the existing city is important, this study focuses on it.

The purpose of this study is to understand the impact of the weather data in various Japanese cities on the performances of solar collector with different sizes, thus the performances of combined system. The cities studied were Kofu city, Nagoya city and Yamagata city. According to the annual ranking on the duration of sunshine for the prefectural capital cities in Japan in 2021 [16], the ranking of Kofu city, Nagoya city and Yamagata city was 1, 24 and 47, respectively. Therefore, this study was thought to cover the most areas in Japan. This study refers the developed heat transfer model investigating PTC [17]. PTC is the most appropriate collector to provide the solar thermal energy at an intermediate temperature range among the several types of concentrating solar collector [18]. The temperature of heat transfer fluid out of the PTC could range approximately 700 K - 873 K [19, 20]. The temperature of heat transfer fluid was calculated by the developed heat transfer model [17] with the weather data of Kofu city, Nagoya city and Yamagata city in Japan in 2021 [21]. This study adopted the specific characteristics of a biogas dry reforming reactor developed by authors to estimate the amount of produced H_2 [22, 23] and the power generated by SOFC with H_2 obtained from biogas dry reforming reactor.

2. Heat Transfer Model for Solar Collector Proposed

2.1. Govering Equation

Preprints.org (www.preprints.org) | NOT PEER-REVIEWED | Posted: 29 January 2024 doi:10.20944/preprints202401.1909.v1

Figure 1 illustrates the schematic drawing for heat transfer model of the PTC proposed in this study. In this model, a solar radiation is mainly absorbed on the outer surface of the absorber tube [17]. Some absorbed heat transports to the heat transfer fluid by conduction through the tube wall and convection from the inner surface of the tube to the fluid (Q_h). Other heat transfers as a loss by radiation to the inner surface of the glass tube through the vacuum space (Q_r) and then by conduction from the inner surface of the glass tube to the outer surface of the glass tube (Q_c). The heat transferred to ambient from the outlet surface of the glass tube by two mechanisms as follows: (i) the convection to the surrounding air (Q_a), (ii) the radiation to the surrounding surfaces (Q_s), e.g. building and sky.

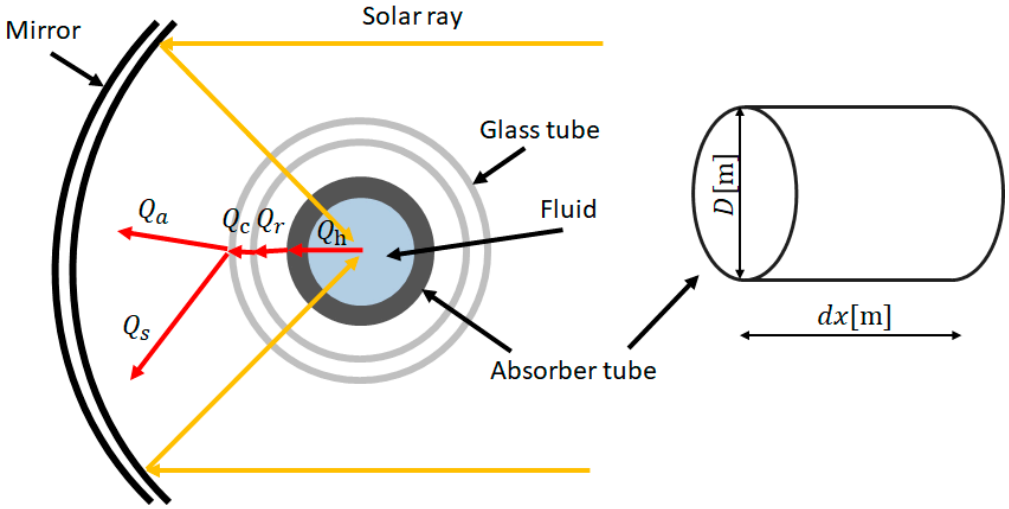

Figure 1. Schematic drawing for heat transfer model of parabolic trough solar collector investigated in this study.

Figure 2 shows the thermal resistance diagram for the heat transfer process in this model. In this model, R_1 indicates the thermal resistance by convection from the heat transfer fluid to the absorber [K/W]. R_2 indicates the thermal resistance by conduction through the absorber [K/W]. R_3 indicates the thermal resistance by radiation through vacuum [K/W]. R_4 indicates the thermal resistance by conduction through the glass tube [K/W]. R_5 indicates the thermal resistance by convection to the ambient air [K/W]. R_6 indicates the thermal resistance by radiation to the surrounding surfaces (buildings and sky).

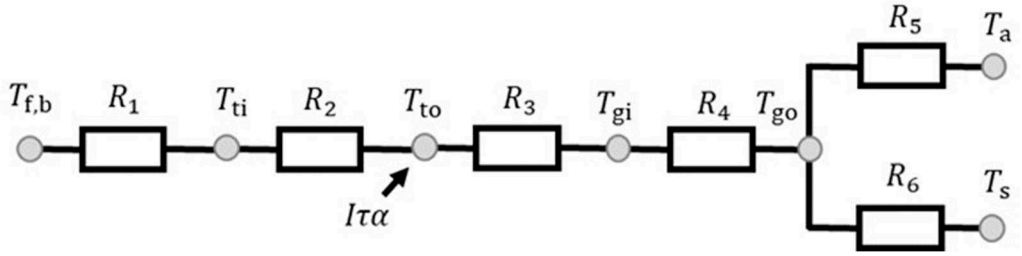

Figure 2. Thermal resistance diagram of heat transfer model investigated in this study.

This study assumes that the surrounding surface temperature is equal to the ambient air temperature. The model equation for a single glass tube can be expressed as follows [17].

$$I\alpha\tau D\pi dx = \frac{T_{to} - T_{fb}}{R_1} + \frac{T_{to} - T_s}{\left(R_5^{-1} + R_6^{-1}\right)^{-1}} \tag{1}$$

$$mc\frac{dT_{fb}}{dx} = mc\frac{T_{fb,out} - T_{fb,in}}{dx} = \frac{T_{to} - T_{fb}}{R_1} \tag{2}$$

$$\frac{T_{to} - T_{gi}}{R_3} = \frac{T_{to} - T_s}{R_3 + \left(R_5^{-1} + R_6^{-1}\right)^{-1}} \tag{3}$$

where I is the solar intensity [W/m²], α is the absorptivity of absorber tube [-], τ is the transmissivity of glass tube [-], D is the diameter of absorber [m], dx is the length of absorber [m], m is the mass flow

Preprints.org (www.preprints.org) | NOT PEER-REVIEWED | Posted: 29 January 2024 doi:10.20944/preprints202401.1909.v1

rate of heat transfer fluid which is assumed to be a biogas [kg/s], c is the specific heat of heat transfer fluid [J/(kg · K)], T_{fb} is the temperature of heat transfer fluid [K], $T_{fb,\,out}$ is the temperature of heat transfer fluid at outlet [K] and $T_{fb,\,in}$ is the temperature of heat transfer fluid at inlet [K]. Each thermal resistance is defined as following:

$$R_1 = \frac{1}{2\pi r_{ti} h} \tag{4}$$

$$R_2 = \frac{1}{2\pi k_t} \ln \frac{r_{to}}{r_{ti}} \tag{5}$$

$$R_3 = \frac{1}{2\pi\sigma r_{to}} \left[\frac{1}{\varepsilon_t} + \frac{1-\varepsilon_g}{\varepsilon_g} \left(\frac{r_{to}}{r_{gi}} \right) \right] \left[\left(T_{to}^2 + T_{gi}^2 \right) \left(T_{to} + T_{gi} \right) \right]^{-1} \tag{6}$$

$$R_4 = \frac{1}{2\pi k_g} \ln \frac{r_{go}}{r_{gi}} \tag{7}$$

$$R_5 = \frac{1}{2\pi r_{go} h_o} \tag{8}$$

$$R_6 = \frac{1}{\varepsilon_g \sigma 2\pi r_{go} \left(T_{go} + T_s \right) \left(T_{go}^2 + T_s^2 \right)} \tag{9}$$

where r_{ti} is the inner radius of absorber [m], r_{to} is the outer radius of absorber [m], r_{gi} is the inner radius of glass tube [m], r_{go} is the outer radius of glass tube [m], σ is Stefan-Boltzmann constant [W/(m² · K⁴)], h is the heat transfer coefficient between the heat transfer fluid and the inner surface of absorber [W/(m² · K)], h_o is the heat transfer coefficient from the outer surface of glass tube to atmosphere [W/(m² · K)], k_t is the thermal conductivity of absorber [W/(m · K)], k_g is the thermal conductivity of glass tube [W/(m · K)], ε_t is the emissivity of absorber [-], ε_g is the emissivity of glass tube [-], T_{to} is the temperature of outer surface of absorber [K], T_{gi} is the temperature of inner surface of glass tube [K], T_{go} is the temperature of outer surface of glass tube [K], T_s is the temperature of surrounding surface [K] and T_a is the temperature of surrounding air [K].

2.2. Estimation of Heat Transfer Coefficient

The convective heat transfer coefficient for the turbulent flow in a tube was estimated by Dittus-Boelter correlations [24] in this study as follows:

$$Nu = 0.023\,\mathrm{Re}^{0.8}\,\mathrm{Pr}^{1/3} \tag{10}$$

$$Nu = \frac{hD}{k_a} \tag{11}$$

$$\mathrm{Re} = \frac{\rho_a u_a D}{\mu_a} \tag{12}$$

$$\mathrm{Pr} = \frac{C_{p,a}\mu_a}{k_a} \tag{13}$$

$$h_o = 0.0191 + 0.006608 u_a \tag{14}$$

where $C_{p,\,a}$ is the specific heat of surrounding air [J/(kg · K)], μ_a is the viscosity [Pa · s], k_a is the thermal conductivity of surrounding air [W/(m · K)], u_a is the velocity of surrounding air [m/s] and ρ_a is the density of surrounding air [m/s].*1.3. Calculation procedure*

According to Equations (1) and (2), the following equation can be drawn:

$$T_{fb,out} = \frac{dx}{mc} \left\{ I\alpha\tau D\pi dx - \frac{\left(T_{to} - T_s \right)\left(R_5 + R_6 \right)}{R_3\left(R_5 + R_6 \right) + R_5 R_6} \right\} + T_{fb,in} \tag{15}$$

Moreover, R_3 is decided from Equation (3) as follows:

$$R_3 = \frac{\left(T_{to} - T_{gi} \right) R_5 R_6}{\left(R_5 + R_6 \right)\left(-T_s + T_{gi} \right)} \tag{16}$$

According to Equations (6) and (16), T_{to} can be obtained as follows:

Preprints.org (www.preprints.org) | NOT PEER-REVIEWED | Posted: 29 January 2024 doi:10.20944/preprints202401.1909.v1

$$T_{to} = \left[\frac{(R_5 + R_6)(-T_s + T_g)}{2\pi\sigma t_{to} R_5 R_6} \times \frac{\{r_{gi} + r_{to}(1-\varepsilon_g)\}}{\varepsilon_t r_{gi}} + T_{gi}^4 \right]^{\frac{1}{4}} \quad (17)$$

T_{fb} is calculated by averaging $T_{fb,\,in}$ and $T_{fb,\,out}$ as follows:

$$T_{fb} = \frac{T_{fb,in} + T_{fb,out}}{2} \quad (18)$$

In this study, T_{fb} is calculated changing dx according to the above equations. This study set D = 1.5 m according to the optimization by the authors' previous study [6]. The weather data, i.e. I, u_a and T_a in Kofu city, Nagoya city and Yamagata city are inputted [21]. The heat transfer fluid is assumed as the mixture of CH_4 and CO_2. The molar ratio of CH_4 : CO_2 is 1.5 : 1, which simulates the biogas. The following assumptions are considered in this study:

(i) The mass flow rate of the heat transfer fluid (m) is 0.05 kg/s.
(ii) The distance between absorber and glass tube is 1/10 D.
(iii) $T_{fb,\,in}$ is 283 K.
(iv) T_s equals to T_a.
(v) The thickness of absorber and glass tube is 0.005 m and 0.010 m, respectively.
(vi) R_2 and R_4 are ignored since they are very small compared to the other thermal resistances [17].
(vii) T_{ti} equals to T_{to}.
(viii) T_{gi} equals to T_{go}, which is 373 K.

Table 1 lists the values of physical properties adopted in this study.

Table 1. The values of physical properties adopted in this study. [17, 25].

Property	Value	Information
α [-]	0.94	-
τ [-]	0.94	-
ε_t [-]	0.9	-
c [J/(kg・K)]	1.335	for CH_4:CO_2 = 1.5:1
σ [W/(m²・K⁴)]	5.67×10^{-8}	Stefan-Boltzmann coefficient
ε_g [-]	0.94	Glass smooth surface
k_a [W/(m・K)]	0.0257	Surrounding air
ρ_a [kg/m³]	1.166	Surrounding air
μ_a [Pa・s]	1.82×10^{-5}	Surrounding air
$C_{p,a}$ [J/(kg・K)]	1006	Surrounding air
k_t [W/(m・K)]	16	Stainless steel
K_g [W/(m・K)]	1.3	Quartz glass

3. Proposed Combined Energy System

Figure 3 illustrates the proposed system consisting of solar collector, biogas dry reforming reactor and SOFC proposed [6]. In the proposed system, the heat transfer fluid consisting of CH_4 and CO_2 flows into solar collector. After heated by solar collector, the heat transfer fluid flows into biogas dry reforming reactor. H_2 is produced in the reactor through biogas dry reforming process. The produced H_2 is supplied into SOFC as a fuel, resulting that the electricity is generated. The by-product of the process, CO was not considered in this study.

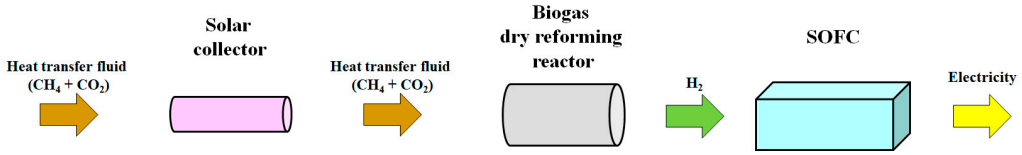

Figure 3. System consisting of solar collector, biogas dry reforming reactor and SOFC proposed by this study.

Preprints.org (www.preprints.org) | NOT PEER-REVIEWED | Posted: 29 January 2024 doi:10.20944/preprints202401.1909.v1

To calculate the amount of H_2 produced from the biogas dry reforming reactor, this study follows the reaction scheme of biogas dry reforming as follows:

$$CH_4 + CO_2 \rightarrow 2H_2 + 2CO \quad (19)$$

In this study, the molar flow rate of CO_2 and CH_4 is 1.67×10^{-2} mol/s and 2.51×10^{-2} mol/s, respectively. This molar ratio represents CH_4 : CO_2 of 1.5 : 1 when m is 0.05 kg/s. According to Equation (19) and these molar flow rates, the molar flow rate of produced H_2 can be calculated to be 3.34×10^{-2} mol/s. From the authors' previous experimental studies changing the reaction temperature, which corresponds to T_{fb} in this study, from 673 K to 873 K [22, 23], the performance of biogas dry reforming is the best at 873 K. Therefore, this study assumes that H_2 can be produced by biogas dry reforming at T_{fb} over 873 K. The conversion ratio of H_2 is assumed to be 100 %. Though the highest conversion ratio of H_2 was approximately 10 % according to the authors' previous experimental studies [22, 23], this study assumes that the conversion ratio of H_2 is 100 % as the ideal maximum performance case.

To estimate the power generated by SOFC, this study considers the lower heating value of H_2 (= 10.79 MJ/m^3_N) and the power generation efficiency of commercial SOFC of 55 % [25]. When the conversion ratio of H_2 is 100 %, the power generated by SOFC can be calculated as follows:

$$(3.34\times10^{-2}\ [mol/s]\times22.4\ [L/mol])\div(1000\ [L/m^3]\times0.55\times(10.79\ [MJ/(m^3N)])= 4.44\ [kW] \quad (20)$$

The amount of produced H_2 and the power generated by SOFC which are estimated by this study under several conditions are discussed in the next section.

4. Results and Discussion

4.1. Temperature of Heat Transfer Fluid

The weather data of I, u_a and T_a in Kofu city, Nagoya city and Yamagata city in 2021 [21] which are adopted for the calculation of T_{fb} were collected and are shown in **Tables 2–4**. As representative data for each city, the data in January are shown in these tables. The monthly mean value of I, u_a and T_a are listed in these tables.

Table 2. Weather data of I, u_a and T_a in Kofu city in January.

Time	I [MJ/m²]	u_a [m/s]	T_a [K]
6:00	0	1.5	272.6
7:00	0.6	1.6	272.4
8:00	53.4	1.4	273.3
9:00	186.2	1.6	275.0
10:00	316.6	1.7	276.7
11:00	427.1	2.0	278.4
12:00	478.4	2.5	279.8
13:00	472.3	2.6	280.9
14:00	401.3	2.9	281.5
15:00	287.0	3.1	281.6
16:00	157.7	2.9	281.1
17:00	35.2	3.1	279.9
18:00	0.1	3.1	279.9
19:00	0	2.5	277.9

Table 3. Weather data of I, u_a and T_a in Nagoya city in January.

Time	I [MJ/m²]	u_a [m/s]	T_a [K]
6:00	0	2.1	275.4
7:00	0	2.2	275.3
8:00	43.8	2.2	275.8
9:00	166.6	2.4	277.0
10:00	295.3	2.7	278.4

Preprints.org (www.preprints.org) | NOT PEER-REVIEWED | Posted: 29 January 2024 doi:10.20944/preprints202401.1909.v1

11:00	379.0	3.4	279.5
12:00	398.4	3.6	280.3
13:00	422.5	3.8	280.6
14:00	369.0	3.9	281.0
15:00	288.3	3.9	280.9
16:00	168.7	4.0	280.4
17:00	46.8	3.5	279.7
18:00	0.6	3.2	279.0
19:00	0	2.8	278.5

Table 4. Weather data of I, u_a and T_a in Yamagata city in January.

Time	I [MJ/m^2]	u_a [m/s]	T_a [K]
6:00	0	1.4	270.5
7:00	0.2	1.4	270.4
8:00	37.5	1.5	270.8
9:00	134.3	1.5	271.6
10:00	236.3	1.6	272.5
11:00	289.1	1.8	272.9
12:00	320.7	1.6	273.3
13:00	331.9	1.6	273.9
14:00	288.6	1.6	274.2
15:00	186.7	1.6	274.1
16:00	97.8	1.6	273.8
17:00	17.0	1.9	273.1
18:00	0	1.7	272.6
19:00	0	1.6	272.4

Figures 4–7 show the changes of T_{fb} with time in different months and cities. The data in January, April, July and October are shown as a representative data for Winter, Spring, Summer and Autumn, respectively. The monthly mean values are shown in these figures.

Preprints.org (www.preprints.org) | NOT PEER-REVIEWED | Posted: 29 January 2024 doi:10.20944/preprints202401.1909.v1

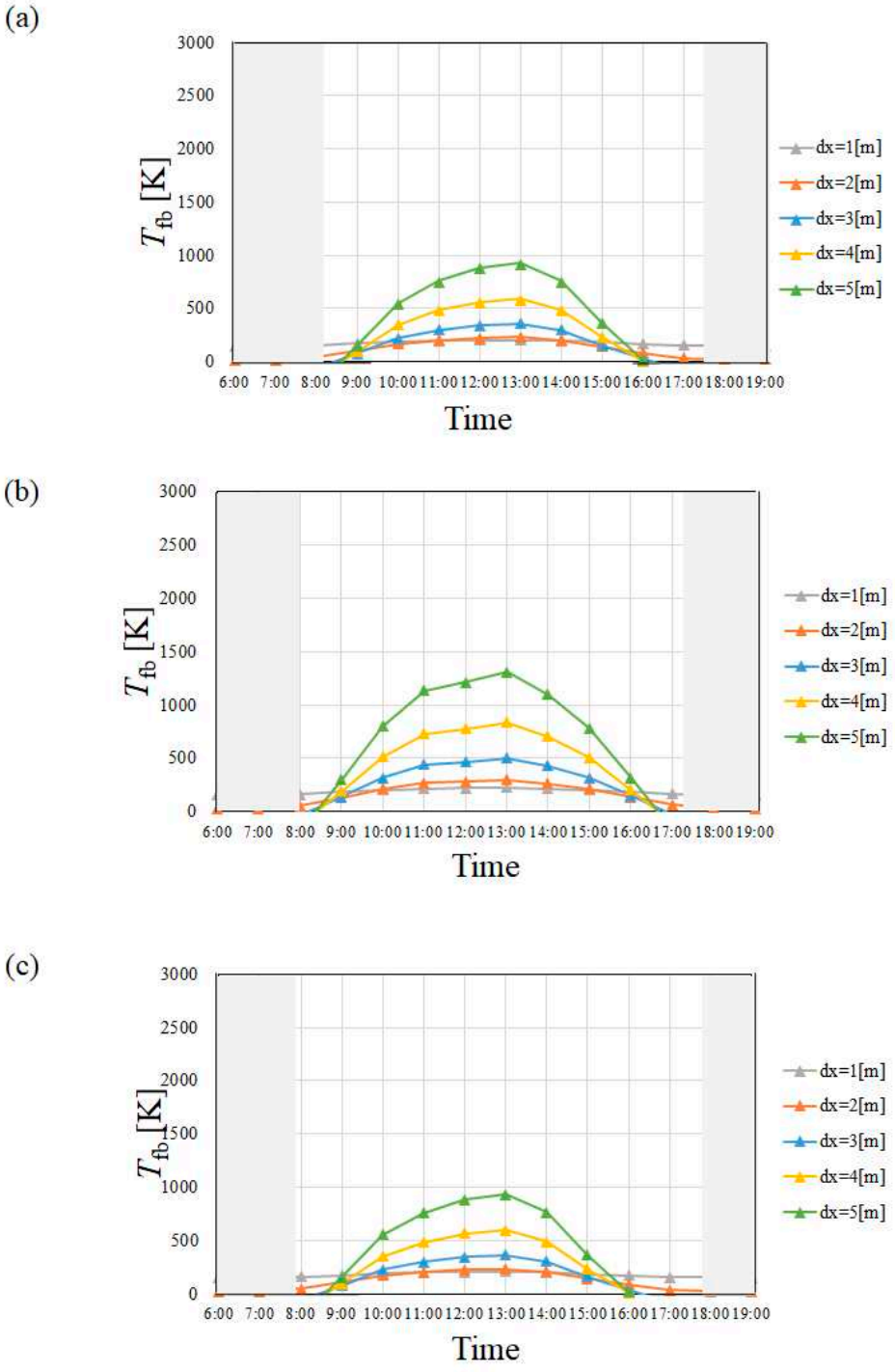

Figure 4. Change of T_{fb} with time among different cities in January ((a): Kofu city, (b): Nagoya city, (c): Yamagata city).

Preprints.org (www.preprints.org) | NOT PEER-REVIEWED | Posted: 29 January 2024 doi:10.20944/preprints202401.1909.v1

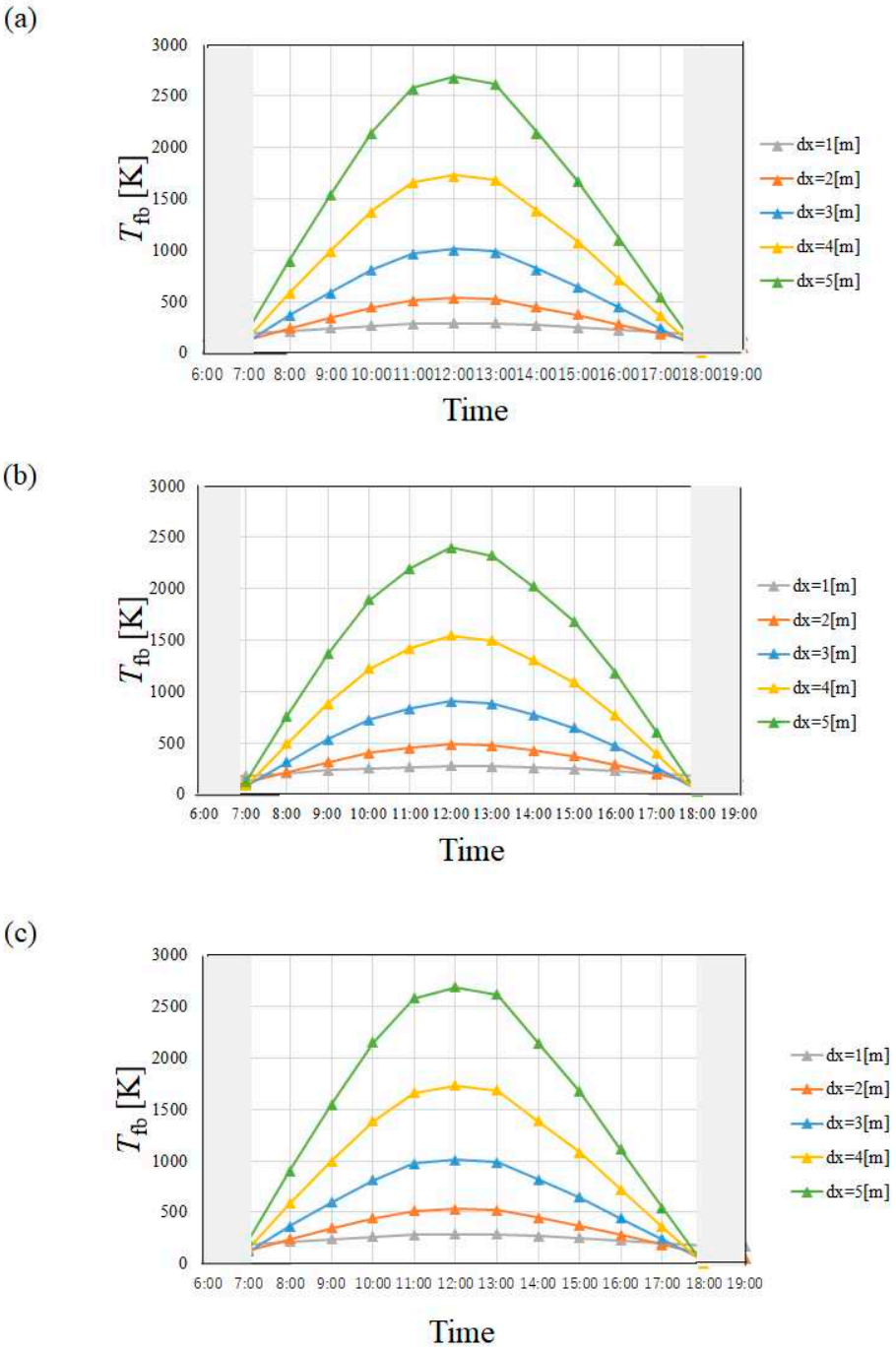

Figure 5. Change of T_{fb} with time among different cities in April ((a): Kofu city, (b): Nagoya city, (c): Yamagata city).

Preprints.org (www.preprints.org) | NOT PEER-REVIEWED | Posted: 29 January 2024 doi:10.20944/preprints202401.1909.v1

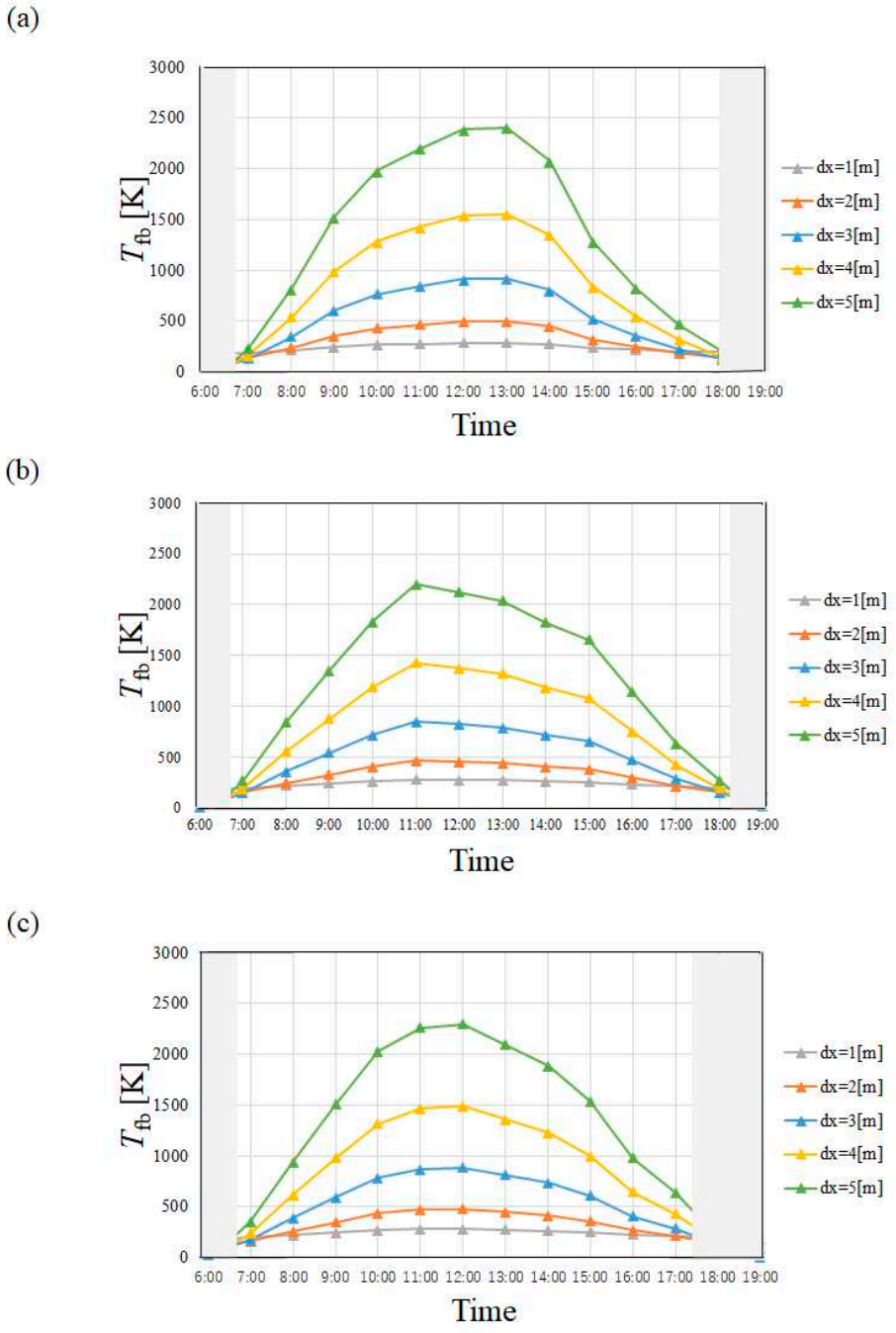

Figure 6. Change of T_{fb} with time among different cities in July ((a): Kofu city, (b): Nagoya city, (c): Yamagata city).

Preprints.org (www.preprints.org) | NOT PEER-REVIEWED | Posted: 29 January 2024 doi:10.20944/preprints202401.1909.v1

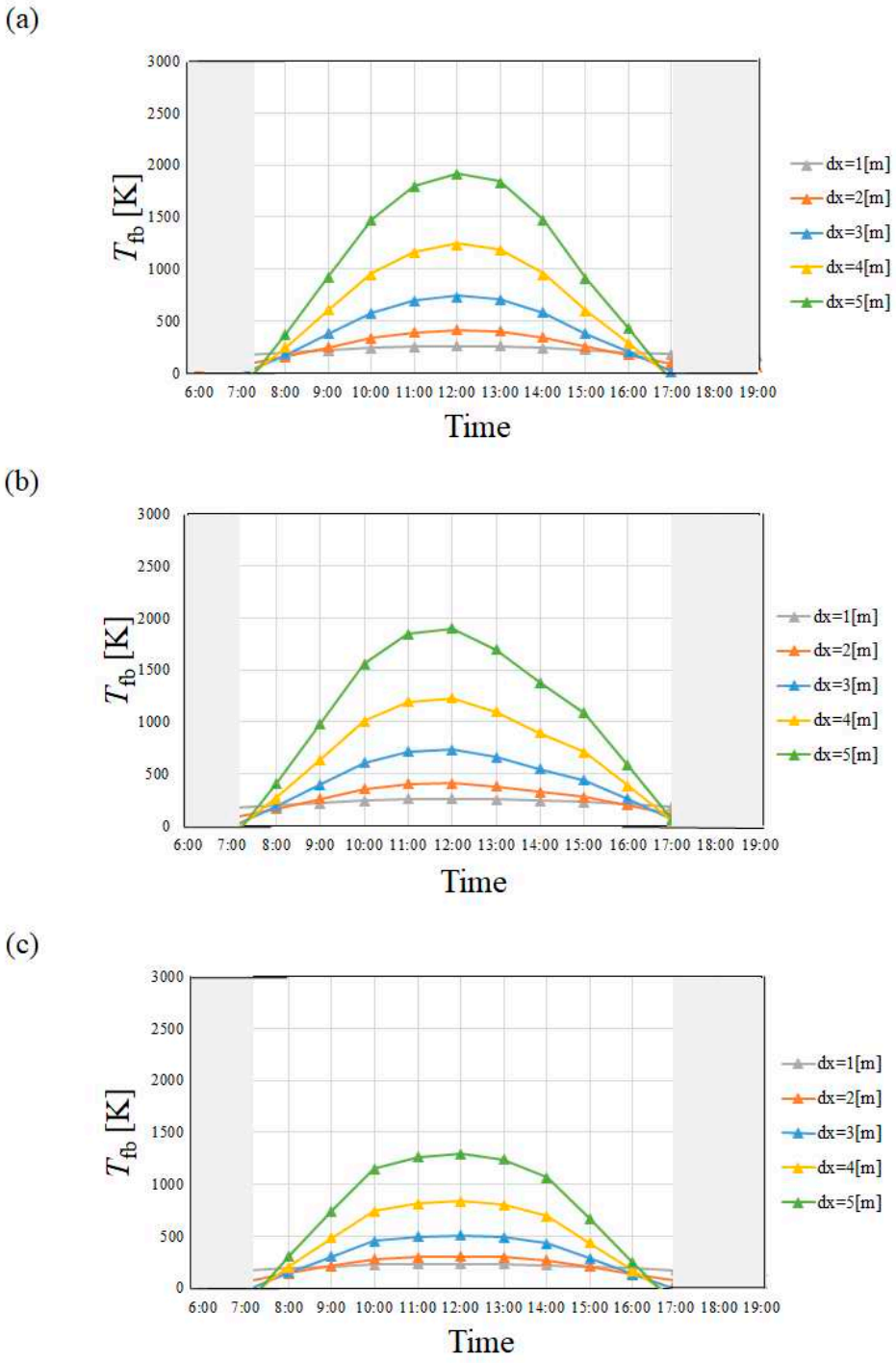

Figure 7. Change of T_{fb} with time among different cities in October ((a): Kofu city, (b): Nagoya city, (c): Yamagata city).

It can be seen from **Tables 2–4** and **Figures 4–7** that the change of T_{fb} with time follows the change of I mainly. In addition, T_{fb} in April and July is higher than that in January and October irrespective of city since I in April and July is higher than that in January and October. It is found from **Figures 4–7** that T_{fb} increases with the increase in dx since the surface area of absorber tube, i.e. heat transfer area is larger. Additionally, it can be seen that T_{fb} for dx = 5 m is higher than 2,000 K in April and July irrespective of city, which is not suitable for actual application due to the safety issues of the material of absorber tube. Therefore, this study decides that the optimum dx should be around 4 m irrespective of city to ensure the safety of stainless steel that is the material used to make the absorber tube. For example, the melt point of SUS 405 is 1,700 K [26]. In the following discussion on

Preprints.org (www.preprints.org) | NOT PEER-REVIEWED | Posted: 29 January 2024 doi:10.20944/preprints202401.1909.v1

the analysis results, this study adopts the results using dx = 4 m. As to the comparison of the tendency of T_{fb}, it is seen that T_{fb} in Yamagata city in January and October, i.e. winter and autumn is lower than that in Kofu city and Nagoya city especially, which is influenced by the tendency of I strongly, not u_a. On the other hand, T_{fb} is almost the same in April and July, i.e. spring and summer, irrespective of city. The difference of T_{fb} between Kofu city and Nagoya city is relatively small, resulting from that the difference of duration of sunshine for the ranking prefectural capital city which was under 24 in Japan in 2021 [16].

3.2. Amount of H_2 Produced from Biogas Dry Reforming and Power Generated by SOFC

To calculate the amount of H_2 produced from the biogas dry reforming reactor, **Table 5** lists the time when T_{fb} is over 873 K for Kofu city, Nagoya city and Yamagata city. In this table, the data in the case of dx = 4 m are shown. As we described before, this study assumes that H_2 can be produced at the conversion ratio of H_2 of 100 % when T_{fb} is over 873 K. The time when T_{fb} is over 873 K is marked in this table.

Table 5. The time when T_{fb} is over 873 K for Kofu city, Nagoya city and Yamagata city.

Kofu city												
	7:00	8:00	9:00	10:00	11:00	12:00	13:00	14:00	15:00	16:00	17:00	18:00
Jan					✓	✓	✓	✓				
Feb				✓	✓	✓	✓	✓	✓			
Mar			✓	✓	✓	✓	✓	✓	✓			
Apr			✓	✓	✓	✓	✓	✓	✓	✓		
May			✓	✓	✓	✓	✓	✓	✓	✓		
Jun		✓	✓	✓	✓	✓	✓	✓	✓	✓		
Jul			✓	✓	✓	✓	✓	✓	✓			
Aug			✓	✓	✓	✓	✓	✓	✓	✓		
Sep			✓	✓	✓	✓	✓	✓	✓			
Oct				✓	✓	✓	✓	✓				
Nov				✓	✓	✓	✓	✓				
Dec				✓	✓	✓	✓	✓				
Nagoya city												
	7:00	8:00	9:00	10:00	11:00	12:00	13:00	14:00	15:00	16:00	17:00	18:00

Preprints.org (www.preprints.org) | NOT PEER-REVIEWED | Posted: 29 January 2024 doi:10.20944/preprints202401.1909.v1

Jan					✓	✓	✓	✓				
Feb				✓	✓	✓	✓	✓	✓			
Mar			✓	✓	✓	✓	✓	✓	✓			
Apr			✓	✓	✓	✓	✓	✓	✓	✓		
May			✓	✓	✓	✓	✓	✓	✓			
Jun			✓	✓	✓	✓	✓	✓	✓	✓		
Jul			✓	✓	✓	✓	✓	✓	✓	✓		
Aug			✓	✓	✓	✓	✓	✓	✓	✓		
Sep			✓	✓	✓	✓	✓	✓	✓			
Oct			✓	✓	✓	✓	✓	✓	✓			
Nov				✓	✓	✓	✓	✓				
Dec					✓	✓	✓	✓				

Yamagata city

	7:00	8:00	9:00	10:00	11:00	12:00	13:00	14:00	15:00	16:00	17:00	18:00
Jan												
Feb					✓	✓	✓					
Mar				✓	✓	✓	✓	✓	✓			
Apr			✓	✓	✓	✓	✓	✓	✓	✓		
May			✓	✓	✓	✓	✓	✓	✓			
Jun		✓	✓	✓	✓	✓	✓	✓	✓	✓		
Jul		✓	✓	✓	✓	✓	✓	✓	✓	✓		
Aug			✓	✓	✓	✓	✓	✓	✓			
Sep			✓	✓	✓	✓	✓	✓	✓			

Preprints.org (www.preprints.org) | NOT PEER-REVIEWED | Posted: 29 January 2024 doi:10.20944/preprints202401.1909.v1

Oct		✓	✓	✓	✓	✓
Nov			✓	✓		
Dec						

According to **Table 5**, the time when T_{fb} is over 873 K in spring and summer is longer than that in winter and autumn irrespective of city. This is mainly due to the tendency of I, not u_a. In addition, it is known the time when T_{fb} is over 873 K is 0 in January and December in Yamagata city. Therefore, other cities should be selected if the proposed system would be used all year around.

Table 6 lists the amount of H_2 produced from the biogas dry reforming reactor for Kofu city, Nagoya city and Yamagata city, respectively. It can be seen form **Table 6** that the annual amount of H_2 produced from the biogas dry reforming reactor for Nagoya city is over than that for Kofu city. As described above, the difference of duration of sunshine for the ranking prefectural capital city which was under 24 in Japan in 2021 [16] was small.

Table 6. The amount of H_2 produced from the biogas dry reforming reactor for Kofu city, Nagoya city and Yamagata city.

	Kofu city [kg]	Nagoya city [kg]	Yamagata city [kg]
Jan	29.82	29.82	0
Feb	40.40	40.40	20.20
Mar52.18	52.18	52.18	37.27
Apr	57.72	57.72	57.72
May	59.64	52.18	52.18
Jun	64.93	57.72	61.93
Jul	52.18	59.64	67.09
Aug	59.64	74.55	52.18
Sep	50.50	50.50	50.50
Oct	44.73	52.18	37.27
Nov	36.07	36.07	36.07
Dec	37.27	29.82	0

It is seen from **Table 6** that the amount of produced H_2 from the biogas dry reforming reactor in spring and summer is higher as expected, compared to the other seasons irrespective of city. This could be explained by the time when T_{fb} is over 873 K listed in **Table 5**.

Table 7 lists the power generated by SOFC with the H_2 generated from the biogas dry reforming reactor for Kofu city, Nagoya city and Yamagata city. The annual power generated by SOFC for Kofu city, Nagoya city and Yamagata city is 10,809 kWh, 10,959 kWh and 8,389 kWh, respectively. The annual power generated by SOFC for Nagoya city was also higher than that for Kofu city. As described above, the difference of duration of sunshine for the ranking prefectural capital city which was under 24 in Japan in 2021 [16] was small.

Table 7. The power generated by SOFC for Kofu city, Nagoya city and Yamagata city.

	Kofu city [kWh]	Nagoya city [kWh]	Yamagata city [kWh]
Jan	551	551	0
Feb	746	746	373
Mar52.18	964	964	689
Apr	1070	1070	1070
May	1100	964	964
Jun	1200	1070	1200
Jul	964	1100	1240

Preprints.org (www.preprints.org) | NOT PEER-REVIEWED | Posted: 29 January 2024 doi:10.20944/preprints202401.1909.v1

Aug	1100	1380	964
Sep	933	933	933
Oct	826	964	689
Nov	666	666	267
Dec	689	551	0

It is seen from **Table 7** that the power generated by SOFC in spring and summer is higher compared to the other seasons irrespective of city, which can be explained by the time when T_{fb} is over 873 K in **Table 5**. In addition, it is found from **Table 7** that the power generated by SOFC in January and December in Yamagata city is 0, because the reactor did not work as T_{fb} was lower than 873 K. Therefore, as claimed before, other cities should be selected if the proposed system would be used all year around.

Table 8 lists the number of households whose power demand could be met by the combined system in each month for Kofu city, Nagoya city and Yamagata city. The number that was termed as "available households number per month" in this study, was calculated by dividing the power generated by SOFC by the electricity demand of couple households in each season [27].

Table 8. The available households number per month for Kofu city, Nagoya city and Yamagata city.

	Kofu city [-]	Nagoya city [-]	Yamagata city [-]
Jan	1.7	1.7	0
Feb	2.6	2.6	1.3
Mar52.18	4.0	4.0	2.9
Apr	4.6	4.6	4.6
May	4.6	4.0	4.0
Jun	4.7	4.2	4.7
Jul	3.7	4.2	4.7
Aug	4.2	4.2	3.7
Sep	4.0	4.0	4.0
Oct	3.5	4.0	2.9
Nov	2.8	2.8	1.1
Dec	2.1	1.7	0

It can be seen from **Table 8** that the highest available households number per month clarified in this study is 4.7 in June in Kofu. According to **Table 8**, this highest number can be also observed for Yamagata city. In spring and summer in Yamagata city, the foehn phenomenon, which causes the sunny days with high temperature, seldom occurs [21]. Therefore, the highest available household number per month of 4.7 can be obtained even for Yamagata city. However, the highest available households number per month of 4.7 is still small. In this study, the analysis was conducted for the case of m = 0.05 kg/s. If m was larger, the amount of H_2 produced from the biogas dry reforming reactor would increase. The optimum dx and D would be changed when m was over 0.05 kg/s. In addition, the available households number per month was small in autumn and winter. To supply the energy for these seasons, the storage of H_2 after a biogas dry reforming is proposed and is being studied currently. The results on these subjects will be reported in the near future.

4. Conclusions

This study has simulated the performances of PTC and a proposed energy system with the weather data of different cities in Japan. The cities studied were Kofu city, Nagoya city and Yamagata city which almost cover the whole climate zones of Japan. The temperature of heat transfer fluid was calculated by the simple but effective heat transfer model developed. The following conclusions could be drawn from the study:

1. T_{fb} in April and July is higher than that in January and October irrespective of city since I in April and July is higher than that in January and October.

Preprints.org (www.preprints.org) | NOT PEER-REVIEWED | Posted: 29 January 2024 doi:10.20944/preprints202401.1909.v1

2. T_{fb} increases with the increase in dx. However, this study has decided that the optimum and maximum dx should be 4 m irrespective of city since this study assumed to use stainless steel as the material to make the absorber tube.
3. T_{fb} in Yamagata city in January and October, i.e. winter and autumn was lower than that in Kofu city and Nagoya city especially, which is influenced by the tendency of I strongly, not u_a. On the other hand, T_{fb} was almost the same in April and July, i.e. spring and summer, irrespective of city.
4. The amount of produced H_2 as well as the power generated by SOFC in spring and summer were higher compared to the other seasons irrespective of city.
5. The highest available households number per month found in this study was 4.7 in June in Kofu city as well as June and July in Yamagata city. To increase the households number, some measures, e.g. increasing m should be further studied.

Author Contributions: Conceptualization and writing—original draft preparation, A.N.; methodology, R.S.; writing—review and editing, E. H.; All authors have read and agreed to the published version of the manuscript.

Funding: Please add: This research was funded by Mie University.

Conflicts of Interest: The authors declare no conflicts of interest.

References

1. Agency for Natural Resources and Energy, Energy White Paper 2023. Available online: https://www.ebecgi.meti.go.jp/about/whitepaper/2023/pdf/ (23 January 2024).
2. International Energy Agency, World Energy Outlook 2022. Available online: https://www.jea.org/reports/world-energy-outlook-2022/outlook-for-electricity (23 January 2024).
3. Jelle, B. P. Building integrated photovoltaics: a concise research pathways. *Energies* **2016**, *9*, doi:10.3390/en9010021.
4. World Bioenergy Association, Global Bioenergy Statistics. Available online: https://worldbioenergy.org/uploads/221223%20WBA%20GBS202022.pdf (23 January 2024).
5. Mao, C.; Chen, S.; Shang, K.; Liang, L.; Ouyang, J. Highly active Ni-Ru bimetallic catalyst integrated with MFI zeolite-loaded cerium zirconium oxide for dry reforming of methane. *ACS Applied Material & Interfaces* **2022**, *14*, 47616-47632.
6. Nishimura, A.; Sato, R.; Hu, E. An energy production system powered by solar heat with biogas dry reforming reactor and solid oxide fuel cell. *Smart Grid and Renewable Energy* **2023**, *14*, 85-106.
7. Zhang, T.; Tang, X. Y.; Yang, W. W.; Ma, X. Comprehensive performance study on reflux solar methanol stream reforming reactor for hydrogen production. *International Journal of Hydrogen Energy* **2023**, *48*, 879-893.
8. Lu, B.; Liu, T.; Yan, X.; Zheng, Z; Liu, Q. A new solar mid-and-low temperature receiver/reactor with linear Fresnel reflector. *Applied Thermal Engineering* **2023**, *226*, doi:10.1016/j.applthermaleng.2023.120216.
9. Sarabchi, N.; Yari, M.; Mahmoudi, S. M. S. Exergy and exergoeconomic analysis of novel high-temperature proton exchange membrane fuel cell based combined cogeneration cycles, including methanol steam reformer integrated with catalytic combustor or parabolic trough solar collector. *Journal of Power Sources* **2021**, *485*, doi:10.1016/j.jpowsour.2020.229277.
10. Cheng, Z. D.; Leng, Y. K.; Men, J. J.; He, Y. L. Numerical study on a novel parabolic trough solar receiver-reactor and a new control strategy for continuous and efficient hydrogen production. *Applied Energy* **2023**, *261*, doi:10.1016/j.apenergy.2019.114444.
11. Cheng, Z. D.; Men, J. J.; He, Y. L.; Tao, Y. B.; Ma, Z. Comprehensive study on novel parabolic trough solar receiver-reactors for hydrogen production. *Renewable Energy* **2019**, *143*, 1766-1781.
12. Wang, H.; Liu, M.; Kong, H.; Hao, Y. Thermodynamic analysis on mid-low temperature solar methane steam reforming with hydrogen permeation membrane reactors. *Applied Thermal Engineering* **2019**, *152*, 925-936.
13. Zhao, Q.; Su, B.; Wang, H.; He, A.; He, R.; Kong, H. Mid/low-temperature solar hydrogen generation via dry reforming of methane enhanced in a membrane reactor. *Energy Conversion and Management* **2021**, *240*, doi:10.1016/j.enconman.2021.114254.
14. Fuqiang, W.; Lin, J.; Ziming, C.; Huaxu, L.; Jianyu, T. Combination of thermodynamic analysis and regression analysis for steam and dry methane reforming. *International Journal of Hydrogen Energy* **2019**, *44*, 15795-15810.
15. Rathod, V. P.; Shete, J.; Bhale, P. V. Experimental investigation on biogas reforming to hydrogen rich syngas production using solar energy. *International Journal of Hydrogen Energy* **2016**, *41*, 132-138.
16. Graph to Chart, The Annual Duration of Sunshine for Prefectural Capital Cities in Japan. Available online: https://graphtochart.com/japan/world-yearly-sunshine_hour2.php (23 January 2024).

Preprints.org (www.preprints.org) | NOT PEER-REVIEWED | Posted: 29 January 2024 doi:10.20944/preprints202401.1909.v1

17. Kumar, K. H.; Daabo, A. M.; Karmakar, M. K.; Hirani, H. Solar parabolic dish collector for concentrated solar thermal systems: a review and recommendation. *Environmental Science and Pollution Research* **2022**, *29*, 32335-32367.
18. Kalogirou, S. A. Solar thermal collectors and application. *Prog. Energy Combust. Sci.* **2004**, *30*, 231-295.
19. Badar, R.; Pedretti, A.; Barbato, M.; Steingeld, A. An air-based corrugated cavity-receiver for solar parabolic trough concentrators. *Applied Energy* **2015**, *138*, 337-345.
20. Valladares, O. G.; Velazquez, N. Numerical simulation of parabolic trough solar collector: improvement using counter flow concentric circular heat exchangers. *International Journal of Heat and Mass Transfer* **2009**, *52*, 597-609.
21. Japan Meteorological Agency, Past Meteorological Data Search. Available online: http://www/data/jma.go.jp/obd/stats/etrn/index/php (23 January 2024).
22. Nishimura, A.; Tanaka, T.; Ohata, S.; Kolhe, M. L. Biogas dry reforming for hydrogen through membrane reactor utilizing negative pressure. *Fuels* **2021**, *2*, 191-209.
23. Nishimura, A.; Ohata, S.; Okukura, K.; Hu, E. The impact of operating conditions on the performance of a CH_4 dry reforming membrane reactor for H_2 production. *Journal of Energy and Power Technology* **2020**, *2*, doi:10.21926/jept.2002008.
24. Kreith, F.; Freider, J. K. Preprints of thermodynamics and heat transfer applied to solar energy. *Solar Energy Handbook*, 1st ed.; McGraw-Hill, New York, 1981; p. 1.
25. NEDO (New Energy and Industry Technology Development Organization), Road Map of 2017 of NEDO Fuel Cell and Hydrogen. Available online. https://www.nedo.go.jp/content/100871873.pdf (23 January 2024).
26. The Japan Society of Mechanical Engineers. *JSME Heat Transfer Handbook*, 1st ed.; Maruzen, Tokyo, 1993; p. 371.
27. Power Plan. Available online. https://standard-project.net/energy/stasistis/emegy-consumption-day.html (23 January 2024).

Disclaimer/Publisher's Note: The statements, opinions and data contained in all publications are solely those of the individual author(s) and contributor(s) and not of MDPI and/or the editor(s). MDPI and/or the editor(s) disclaim responsibility for any injury to people or property resulting from any ideas, methods, instructions or products referred to in the content.